CROATICA CHEMICA ACTA CCACAA **65** (2) 425–438 (1992)

ISSN 0011-1643
UDC 541.1
CCA–2068

Original Scientific Paper

Surfactant Aggregation in Organic Solvents: Structural Features of some Physical Gel Networks Probed by Small Angle Neutron Scattering

P. Terech

Institut Laue-Langevin, 156X, 38042, Grenoble (Cédex), France

Received August 6, 1991

We have studied viscoelastic gel-like systems constituted by surfactants in organic solvents. SANS appears to be efficient technique for investigating both the local and long-range structures of the related 3d networks. The basic equations are given for the scattering from the rod-like aggregates encountered in these phases. The aggregation reactions involve mechanisms specific of the surfactant used. A large variety of structural situations has been found. In each case, the polar heads of the surfactants form a polar inner core surrounded by hydrophobic shell constituted by the hydrocarbon chains. The typical mechanical properties of the samples are partly defined by the structure of the junctions in the network: transient entanglements and crystalline microdomains are the extreme cases found in these physical supermolecular organizations.

INTRODUCTION

Surfactants in aqueous solutions are known to aggregate above the critical micellar concentration (*c.m.c.*). Various theories have been used to describe the onset of spontaneous aggregation (for instance the phase separation, the mass action and the multiple equilibrium models.[1] Further, a theoretical framework accounts for the self-assembly of amphiphiles which links together thermodynamics, interaction free energies and geometry.[2] The relationship between the amphiphile structure and the aggregate morphology has been investigated for various biphenyl or azoxybenzene derivatives[3] for which vesicles, rods, tubes and disks have been observed. Micellar aggregates frequently exhibit spherical shapes. In some special cases of ionic surfactants, ellipsoidal (prolate or oblate spheroids) and rod-like aggregates can be obtained. Most often, the presence of alcohol is necessary to observe such deformed structures (the case of *n*-dodecylbetaine[4]). The surfactant and salt concentrations are some of the parameters which can act, respectively, on the growth of rod-shaped micelles from globular micelles and the curvature of the aggregates. The salt and counterion types are also of importance in the process. For cetylpyridinium bromide (CPyBr)[5] and cetylmethylammonium bromide (CTAB), the resulting aggregate is a long and, more or less, flexible

rod. When the surfactant concentration is further increased (threshold volume fraction ϕ^*), the chains overlap and form a transient network with a mesh size ξ. In these conditions where the chains become entangled, the viscoelastic system exhibits behaviors which can be described by the theories used for solutions of long flexible polymer chains in the semidilute range.[6] But, the physical gel networks can be much less impermanent if stronger interactions of the chains can exist in the so-called junction nodes or zones of the solid-like elastic network in the manner of some aqueous macromolecular systems (for instance like maltodextrine gels which contain disc-like crystalline junctions domains with helical structures.[7] Examples of diluted surfactant-based gels of the aqueous type are rare. But, viscoelastic phases formed with surfactants in solution are not restricted to a single class of aqueous solutions.

On the other side, apolar organic solvents like cyclohexane, octane, decalins are of interest for the simplification they provide. Indeed, the low dielectric constant of these organic media allows to keep the surfactants non-dissociated and also guarantees a lack of hydrogen bonding mechanisms from the solvent in contrast to aqueous biological macromolecular gels where these circumstances are currently encountered. The situation is thus considerably clarified, as compared to the salted aqueous systems. Here, only binary systems composed of low-molecular weight amphiphiles and hydrocarbons, which give rise to gel (or jelly) phases, are considered. The interacting aggregates of the gel phases are responsible for non-Newtonian rheological behaviors which are the origin of numerous industrial applications. We exclude from this presentation more sophisticated cases, such as those found with ternary or quaternary mixtures (*i.e.* microemulsions gels). Micellar structures which could be present below ϕ^* are not detailed. Above ϕ^*, typical dimensions of these aggregates are in the colloidal range and rod-like structures are always observed in the selected examples. These materials are dispersed systems where the surfactant concentration is in the range of a few %wt.

The main structural and dynamical properties of the samples arise from the three-dimensional network formed by the aggregates. The networks are either transient or physical, depending on the structure of the junctions constituted either by entanglements or thermoreversible contacts. Concerning the structural approach, the small angle neutron scattering (SANS) is a powerful technique for the investigation of both the local structure of the aggregates and of their long-range correlations. In fact, numerous other techniques can be used to complement the information, such as light scattering and suitable electron microscopy devices while concerning the dynamical studies, both rheological and quasi-elastic light scattering are very efficient techniques. The basic structural questions important for the organogel surfactant-based networks concern both the local structure of the rod-like scatterers (length, rigidity, cross-sectional shape and internal structure, dimensions, molecular weight per unit length, polydispersity and type of the interfaces) and their interactions in the junction zones of the gel network.

ANALYSIS

(a). SANS Theory

In the following,[8,10] only coherent scattering is considered as a collective scattering property of atoms within a structure. The scattering vector Q for an elastic scattering process is given by:

$$\vec{Q} = \vec{k}_1 - \vec{k}_0$$
$$\vec{Q} = \frac{4\pi}{\lambda} \sin\theta \tag{1}$$

θ being half the scattering angle, λ the neutron wavelength and k the wave vectors. The scattered wave is assumed to radiate spherically around the scatterer with the amplitude:

$$A = \frac{A_0}{r} e^{ik_0 r} \sum_i b_i e^{-i\vec{Q}\cdot\vec{r}_i} \tag{2}$$

where the summation is performed over the i atoms of the scatterer distant of r_i from the origin, b_i is the neutron scattering length for isotope i. For small angle scattering (low resolution), the volume v of the scatterer is considered as a continuous medium characterized by the density of neutron scattering lengths.

$$\rho(\vec{r}) = \frac{1}{v} \sum v b_i (\vec{r} - \vec{r}_i) \tag{3}$$

v is large over interatomic distances but small compared to the resolution of the experiment. The small angle scattering is produced by large scale heterogeneities in the sample which produce fluctuations of $\rho(r)$. The scattered amplitude is the Fourier transform of these fluctuations:

$$A(\vec{Q}) = \int_v \Delta\rho(\vec{r}) e^{-i\vec{Q}} \cdot \vec{r} \, d\vec{r} \tag{4}$$

The SANS intensities measure the average of the squared amplitude:

$$I(\vec{Q}) = \langle |A(\vec{Q})|^2 \rangle = \langle A(\vec{Q}) \cdot A^*(\vec{Q}) \rangle$$

$$I(\vec{Q}) = \left\langle \sum_i \sum_j A_i(\vec{Q}) A_j^*(\vec{Q}) e^{i\vec{Q}\cdot\vec{r}_{ij}} \right\rangle \tag{5}$$

The handling of such formalism to treat the problem of the interacting aggregates encountered in the gel phases is not trivial. The separation between interferences arising from isolated long chain scatterers from that of coupled correlations between pairs of scatterers is rarely achieved. In special cases, when the interparticle distances are larger than the particle sizes, simplifications in expression (5) may make it possible to distinguish the self and the pair correlations of the scatterers.

$$I(q) = nF_1^2(q) S(Q)$$
$$S(Q) = 1 + n \int_v g(r) e^{-i\vec{Q}\cdot\vec{r}} d\vec{r} \tag{6}$$

where $g(r)$ is the pair correlation function, n the number density of the scatterers, $F_1^2(Q)$ is the single particle intensity and $S(Q)$ the structure factor.

In the following, the theoretical structure factor for the centres of mass of single-type rod-like particles is given in some simple cases. Additionally, when the number density of aggregates is increased, the excess scattering from the junction zones is clarified for specific examples in restricted Q and concentration ranges.

(b). Special Cases

Considering that the viscoelasticity of gel phases formed with a small amount of surfactant is linked to the existence of a 3d network, it is not surprising that rod-like structures prevail in these conditions. We summarize here the major shapes, chain trajectories and inter-aggregate interactions found in the mentioned examples.

Fibres

The simplest shape for a rod-like aggregate is a long straight and rigid chain (fibre). The calculations of expression (5) for a fibre with a homogeneous circular cross-section leads to separated axial and cross-sectional terms:[8]

$$I(Q) = \left(\frac{\pi L}{Q}\right)\left[A\Delta\rho\,\frac{2J_1(Qr_o)}{Qr_o}\right]^2 \tag{7}$$

$$R_G^2 = \frac{r_o^2}{2}$$

where J_1 is the Bessel function of the first order, L and A are, respectively, the length and the cross-sectional area of the rod and R_G is the cross-sectional radius of gyration. For a rectangular cross-section, the intensity reads:[11]

$$I(Q) = \left(\frac{2L}{Q}\right)\int_0^{2\pi}\left[A\Delta\rho\,\frac{\sin(Qa\cos\varphi)}{Qa\cos\varphi}\cdot\frac{\sin(Qka\sin\varphi)}{Qka\sin\varphi}\right]^2 d\varphi$$

$$R_G^2 = \frac{b^2}{3}\left(1+\frac{1}{k^2}\right) \tag{8}$$

where a and b are, respectively, half the length and width of the rectangular cross-section while $k=b/a$ defines its anisotropy.

The Q^{-1} asymptotic behavior is typical of the rod-like character: the product (QI) is representative of the cross-section intensity. The central part of the cross-section scattering can be developed into a power series so that the cross-sectional radius of gyration can be estimated from:[8]

$$\underset{q\to 0}{(QI)} = (QI)_0\exp(-Q^2R_G^2/2) \tag{9}$$

From the radius of gyration (of the overall aggregate from the I values or of the cross-section from the QI values), hypotheses concerning the shape of the aggregate can be tested as shown in expressions (7,8) assuming centrosymmetric homogeneous aggregates. At $Q=0$, all neutron waves are in phase and the average molecular weight per unit length M_L for identical uncorrelated aggregates can be deduced from the extrapolated cross-sectional intensity $(QI)_o$:

$$(QI)_0 = \pi c \, \Delta b^2 \, M_L \tag{10}$$

c being the rod concentration (g cm^{-3}), M_L the mass per unit length of the rod-like aggregate and Δb (cm/g) the specific contrast given by:

$$\Delta b = b_{AG} - \rho_S v_{AG} \tag{11}$$

where b_{AG} is the specific scattering length of the aggregate (cm/g), v_{AG} its specific volume (cm^3/g) and ρ_s the scattering length per unit volume of the solvent (cm/cm^3).

Chains

If the rod-like aggregate exhibits flexibility, various calculations can be made, depending on the chain trajectory. For very flexible chains, where the distribution in space of the subunits follows a Gaussian statistic, the well-known Debye's formula is found:[9] it is the case of some polymeric chains. But the model of a Gaussian coil is not used with the surfactant aggregates because the local rigidity is often higher than that of freely jointed polymeric chains. Consequently, the model of a persistence chain made up of a filament subjected to a bending procedure is more appropriate.[9] According to the ratio of the contour length L over the persistence length (l) (*i.e.* the average length below which the linear object is considered straight and rigid), the scattering functions of these so-called Kratky-Porod chains are known.[12,13] The remarkable feature of the related structure factors, is the occurrence of a Q^{-2} term.

$$I(Q) = \frac{1}{Q}\left[\frac{\pi}{L} + \frac{2}{3\langle l \rangle L Q}\right] \tag{12}$$

Junction Zones

The number density of the junction zones (or nodes) and the elasticity of the connecting chains determine the elastic modulus of the viscoelastic phases. Rheology (controlled stress and dynamical experiments) provide statistical and dynamical information on the junctions of the networks. From a structural point of view, the contact zones in the proposed examples can be either transient chain entanglements or crystalline microdomains. The related scattering curves exhibit either a Q^{-2} low-Q bump or Bragg diffraction peaks. The corresponding characteristic lengths are then either a correlation length ξ describing a »mesh size« between the chain entanglements or short-range molecular periodicities. The Fourier transform of the Oernstein-Zernike expression of the pair correlation function for the nodes leads to the form:[14]

$$I(Q) = I(0)\left[\frac{1}{1+Q^2\xi^2}\right] \tag{13}$$

From the rheological point of view, on the one hand, the chain entanglements lead to more or less pseudo-plastic materials which slowly flow (jelly) while, on the other hand, crystalline zones are responsible for the yield stress value (*i.e.* the lower yield stress which has to be applied before the flow commences) of the related self-supporting gels described as plastic materials.

(c). SANS Procedure

The analysis of the scattering curves is specified in four Q-regions (see Figure 3). From low to large angles, the corresponding correlation lengths of concern are:

Region I: interparticle interferences domain. A concentration study is often necessary to distinguish the intra-aggregate scattering from the interparticular interferences. Typical correlation length: ξ.

Region II: structure factor domain of a single aggregate. A typical example is the Q^{-1} axial factor of rigid and long rods. Typical correlation length: (l) or L.

Region III: sharp intensity decrease region due to the finite size of the cross-section of the aggregate. The determination of the cross-section parameters can be made in the Q-range, where the condition $1/l < Q < 1/r_0$ is fulfilled. The cross-sectional radius of gyration and the molecular weight per unit length of the rod-like aggregate can be deduced. Typical correlation length: r_0 or k (see (7,8)).

Region IV: for higher Q-values, oscillations typical of the form factor and polydispersity of the cross-section can be superimposed to the so-called Porod asymptotic Q^{-4} behavior. The Porod region is used to determine some characteristics of the interface (surface, sharpness).

$$\frac{S}{v} = \frac{\pi}{K} \lim [Q^4 I(Q)] \qquad (14)$$

K being the invariant defined by: $K = \int_0^\infty Q^2 I(Q) \mathrm{d}Q$

Further, some extra scattering features such as Bragg peaks, can indicate a crystalline ordering within the junction zones. Typical correlation lengths: molecular lengths.

EXPERIMENTAL

Three types of surfactants in cyclohexane were studied: long-chain hydroxy fatty acid, D-homosteroid and binuclear copper tetracarboxylate derivatives. The compounds were prepared as already described.[15-17] The 12-hydroxy stearic acid (HSA) and the steroid (ST) compounds were dissolved by gentle heating in high purity reagent grade cyclohexane from Aldrich (water content less than 0.01%). The solutions set to thermally reversible gels on cooling. The bicopper coor-

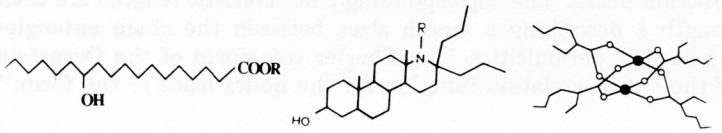

HSA ST Cu-S8

Figure 1. Formulas of the surfactant »gelators«. HSA fatty acid compound where R = H, ST hydroxylated steroid molecule where R = H and bicopper tetracarboxylate Cu-S8 in which the hydrocarbon tail is the branched ethyl-2 hexanoate chain. For Cu-S8, the black full circles represent copper atoms and open circles are oxygen atoms. The molecular shapes are, respectively, roughly elongated, conical and disk-like.

dination complex was dissolved by constant shaking almost without heating and gave blue transparent jellies. This latter system has only thickening properties and the sample slowly flows while for the HSA and ST/cyclohexane systems the samples are self-supporting gels. The critical concentration for the onset of viscoelasticity is typically *ca* 1%wt.

SANS experiments were carried out on instruments D11, D16 and D17 of the high flux reactor of the Institut Laue Langevin (Grenoble, France). The samples were prepared directly in quartz cells of 1.00 mm optical pathlength (irradiated volume is *ca* 60 mm^3). Data calibration was performed by nearly purely incoherent scattering of 1 mm thickness of a light water sample. The momentum transfer was $Q = 4\pi\lambda \sin\theta$, θ being half the scattering angle. We used the facility of rotating the multidetector around the sample to extend the Q-range at larger values (for D16 and D17 spectrometers). We worked with the wavelength corresponding to the maximum of flux available on each of the instruments (D11 and D17) equipped with a Brunhilde velocity selector (triangular distribution FWHM $\Delta\lambda/\lambda$ = 10%). For the D16 spectrometer, the monochromation by a pyrolytic graphite crystal gave a wavelength of 4.5 Å. The Q-range investigated was $0.0008 < Q < 1.0$ $Å^{-1}$. Samples were prepared in deuterated solvents. Corrections were made taking into account the solvent and sample holder backgrounds and transmissions.

STRUCTURAL FEATURES OF ORGANOGEL NETWORKS

In the following, we mention demonstrative examples of surfactant physical organogels, the network structure of which has been investigated by SANS.

(1) Length of the Rod-like Aggregates

Figure 2 shows the scattering curve of a ST gel. The finite size of the overall rod-like scatterer as well as the low-Q limit of the structure factor related to the osmotic compressibility of the gel are far from being probed. Indeed, with the graphic repre-

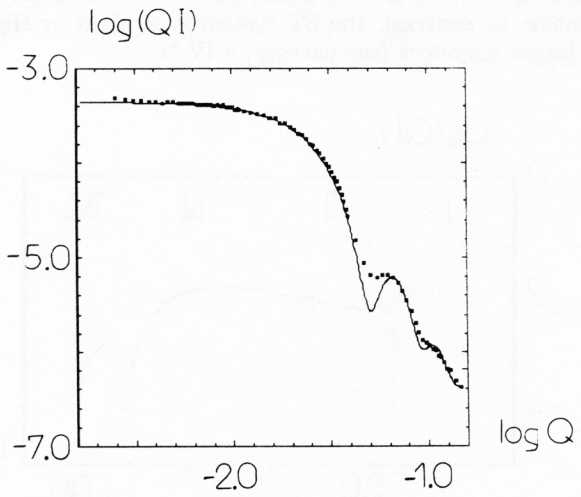

Figure 2. Scattering curve log (QI) *vs.* log Q for the ST/deuterated methyl-cyclohexane system ($c = 2.1\times10^{-2}$ g cm^{-3}). The momentum transfer Q is in $Å^{-1}$ and the intensities I in cm^{-1}. The theoretical adjustment uses expression (7) with r_0 = 78 Å and assuming a Gaussian polydispersity of $\varepsilon = \Delta r_{1/2}/r_{OV} = 0.12$ which includes the experimental resolution.[19]

sentation $\log(Q \cdot I)$ *vs.* $\log Q$, a sharp Gaussian decrease towards zero is expected (see, respectively, Guinier expression (9) for the total intensity of the overall aggregate and the limit of expression (13) at low Q for connected aggregates forming a large network with a meshsize ξ): no such behavior is seen in the experimental Q-range.

The adjustment to the theoretical expression (7) for rigid fibres is satisfactory. We conclude that the aggregates are infinitely long (typically more than *ca.* 5000 Å) over their diameter.[18,19] The inner part of the scattering curve which has been discussed is followed at larger Q-values by a Gaussian exponential decay due to the finite size of the cross-section and by oscillations due to its shape (described by the Bessel function of expression (7). These features are considered in the following paragraphs. Identical conclusions are drawn for the HSA system on the basis of the analysis of the low-angle part of the scattering curve (see Figure 4).

(2) Rigidity of the Rod-like Aggregates

A plot $\log (QI)$ *vs.* $\log Q$ of the cross-sectional intensity exhibits a plateau in the inner part of the scattering curve when the aggregate is straight and rigid (expressions (7,8). Consequently, the ST[18] and HSA[20] gels constituted by very rigid rod-like aggregates (see, respectively, Figure 2 and 4) and the Cu-S8 jellies (Figure 3) described by long flexible chains[21] are two contrasting examples. As shown by expression (12), a Q^{-2} bump in the region I of the scattering curve can be an indication of the flexibility of the chains. A complete study of the scattering curve in the lowest Q-range possible (including the light scattering Q-domain) as a function of the concentration is necessary to assign the bump to the bending specificities of the single particle structure factor. Concerning the Cu-S8 system, complementary work is under progress but as soon as Figure 3 shows such a cross-over between the Q^{-2} and Q^{-1} dependencies of the overall intensity I at $Q \approx 0.007$ Å^{-1} for a jelly at $c = 2.0\times10^{-2}$g cm^{-3}, an estimation of $\langle l \rangle \approx 200$ Å is made. In contrast, the ST system is straight or slightly curvilinear over considerably larger distances (see paragraph IV.1).

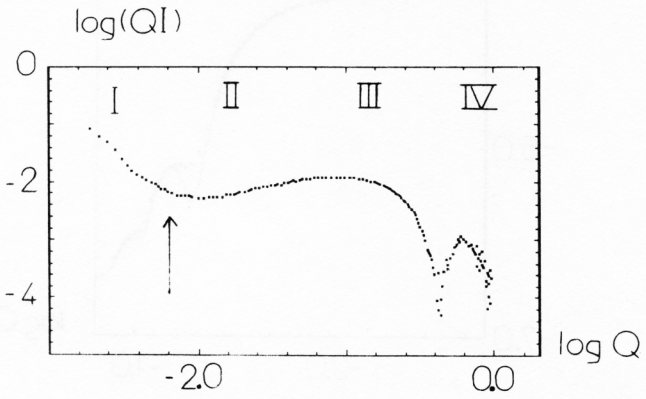

Figure 3. Scattering curve $\log (QI)$ *vs.* $\log Q$ for the Cu-S8/D-cyclohexane system (c = 9.9% wt). The four Q-regions are indicated (see text). The arrow indicates the cross-over between the Q^{-2} and the Q^{-1} behaviors. In region IV, cross-sectional intensity oscillations due to the related form factor in the Porod region are clearly seen.

(3) Cross-section Shapes of the Rod-like Aggregates

A thorough study using the contrast variation method[9,18] allows the assumption that the homogeneous circular cross-section model provides a good adjustment to the experimental data of the ST system (see Figure 2). The HSA fatty acid gels can develop rectangular shapes[22] in given experimental conditions (increase of solvent polarity and/or concentration). Figure 4 presents the variation of the scattering profiles with HSA concentration: the low-angle part clearly evolves from a Q^{-1} towards a Q^{-2} behavior typical of lamellar cross-sectional shapes.[8,9,10]

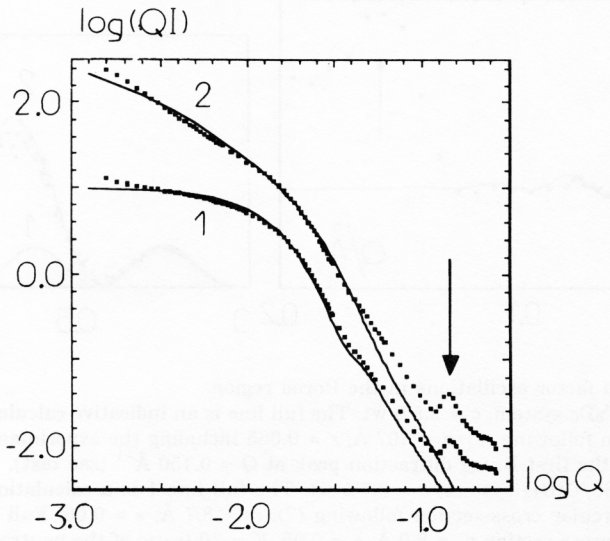

Figure 4. Cross-sectional scattered intensity log (QI) *vs.* log Q: HSA/D-fluorobenzene system (comparable results can be obtained in octane). The arrow indicates the first Bragg diffraction peak at Q *ca.* 0.150 Å^{-1} (see text). Full lines are theoretical adjustments following (8) which do not take into account the Bragg reflections. Curve 1: c = 2.9% wt, b = 120 Å, k = 1, ε = 0.1. Curve 2: c = 11.6% wt, b = 120 Å, k = 0.05, ε = 0.2.

(4) Polydispersity of the Cross-section

The form factor oscillations of region IV are more or less damped according to the polydispersity of the cross-section of the aggregates. Convolution of theoretical expressions (7) or (8) with a normalized Gaussian centered around r_o, smears the secondary minima of the cross-sectional intensity. The ST system, as shown in Figure 2, exhibits well defined oscillations.[20] The geometrical diameter is 99±3 Å. Identically, HSA gels in benzene (comparable results can be obtained in cyclohexane in a given range of concentration) develop fibres with rather monodisperse squared cross-sections, as demonstrated in Figure 5a showing the oscillations in the Porod region. The length of the side is 214±4 Å.

A diameter of 17.6 Å is found[21] for the Cu-S8 aggregates by the use of expression (9) or fits in the Porod region as shown in Figure 5b. These measurements are in agreement with a model of columnar arrangements where the molecules are axially stacked by copper-oxygen coordination bondings (see Figure 1). Refinement of the adjustment is obtained (Figure 5b, curve 2) when the cross-section is considered radially inhomogeneous with respect to the difference of scattering length densities between the inner polar core (copper and oxygen atoms) and the outer hydrophobic shell (hydrocarbon chains).

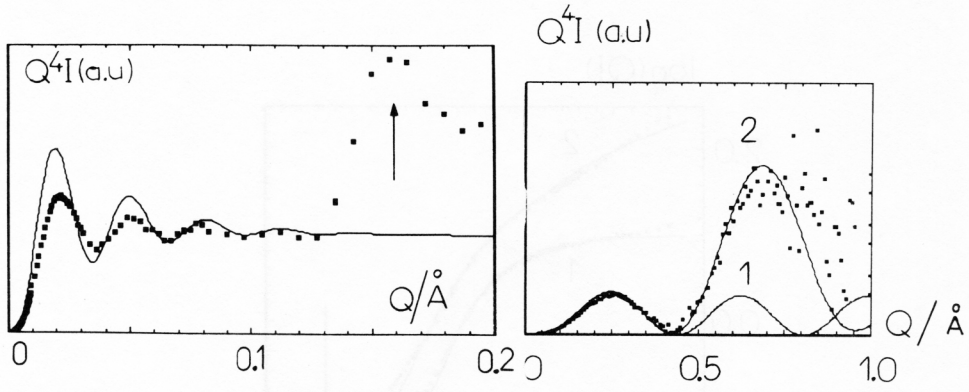

Figures 5. Form factor oscillations in the Porod region.
(a – left): HSA/C_6D_6 system, c = 2.5% wt. The full line is an indicative calculation for fibres with a squared-section following (8): a = 107 Å, ε = 0.065 including the experimental resolution. The arrow indicates the first Bragg diffraction peak at Q = 0.150 $Å^{-1}$ (see text).
(b – right): Cu-S8/C_6D_{12} system, c = 8.7% wt. The full line 1 is a calculation for fibres with a homogeneous circular cross-section following (7): r_o = 8.7 Å, ε = 0.05. Full line 2 concerns an inhomogeneous cross-section r_o = 8.0 Å, ε = 0.05, K = 20 (ratio of the neutron contrast between the inner polar core of radius r = 3 Å and the outer shell of hydrocarbon tails).

(5) Junction Zones

HSA gels in octane develop a crystalline ordering extended in lamellar domains *via* a lateral fibre aggregation process. Bragg peaks (only that at *ca.* 0.150 $Å^{-1}$ is shown) support the assumption of crystalline junctions (Figure 6). The lamellar shapes are evidenced in region I where a typical asymptotic Q^{-2} behavior[9,22] is observed while at large angles, anisotropic Bragg peaks characterize the internal molecular arrangement with respect to the fibre axis. The HSA molecules associate through a collective H bonding process involving the OH groups. The corresponding Bragg distance is compatible with a model where bimolecules are tilted within plane layers.[20,22]

In the ST gels, helical microcrystalline superstructures are involved in the junction zones:[18] Bragg peaks are observed at Q = 0.235 $Å^{-1}$ and Q = 0.432 $Å^{-1}$ (not shown). These structures have also been revealed by freeze-etching replication electron microscopy experiments.[23] In contrast, the Cu-S8 system exhibits a viscoelastic behavior which can be approximated with the Maxwell model used in the description of entangled polymers in semi-dilute solutions.[21] These entanglements require chain flexibility. From a SANS point of view, no Bragg peaks can be detected.

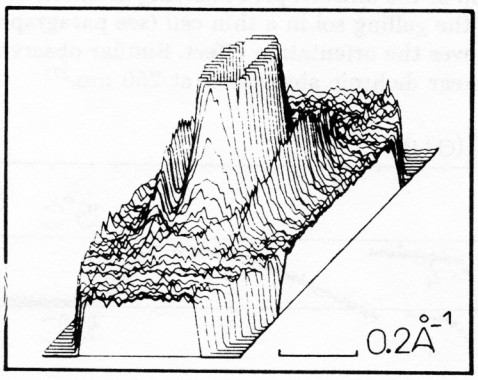

Figure 6. Scattering from the HSA/C_6F_6 system, c = 8.7% wt. The disturbance in the middle is due to the beam stop. An anisotropic Bragg reflection is clearly seen corresponding to a spacing of *ca.* 45 Å in relation with the length of a bimolecule.[22] The central scattering exhibits a Q^{-2} asymptotic behavior typical of lamellar shapes.

(6) Kinetics

The ST gels are obtained after a critical sol → gel transition with characteristic kinetic times ranging from seconds to a few hours. A fraction of the steroid molecules is aggregated within the solid-like gel network while the remainder is constituted by isolated molecules (probed by ESR[24]): it is a supersaturation gel. The temperature affects not only the length of the rod-like aggregates but also the fraction of molecules involved in the aggregation reaction. The sol → gel transition can be studied by SANS: the integrated low-angle part of the overall intensity is proportional to the amount of growing rod-like scatterers (assuming that the shape of the scattering curve does not vary with time in the Q-window of concern). Figure 7 shows an example of the sigmoid curves describing the kinetics of aggregation of the ST molecules in rod-like aggregates.

The Cu-S8 system implies much faster aggregation reactions and can be considered as a two-phase system where the non-aggregated surfactant species are absent. Further, on the basis of dynamical rheology experiments,[21] the dynamics of the Cu-S8 chains could be complicated by additional reactions of scissions and reformations during the reptation of the chains undergoing the shear stress (in the manner of the so-called »living polymers«).[25]

(7) Anisotropies

The two-dimensional detectors used for SANS experiments give information on the orientational behavior of the rod-like aggregates. The anisotropy of the diffraction pattern can be used to analyze the mechanism responsible for the anisotropy of the distribution of the rod axis. Rods can be oriented by means of an electric, magnetic or mechanical (shear gradient) force. With the ST system, anisotropic domains can be observed by the use of strong magnetic fields[26] or shear stresses during the sol → gel transition. The orientation process is effective only during the very first steps of the transition when the growing aggregates are not yet overlapped. Figure 8 shows an ex-

ample of a contour map of the anisotropic scattering intensity obtained for a gel slightly sheared by pouring the gelling sol in a thin cell (see paragraph III). Diminishing the width of the cell improves the orientation effect. Similar observations have been made with records of the linear dichroic absorption at 250 nm.[27]

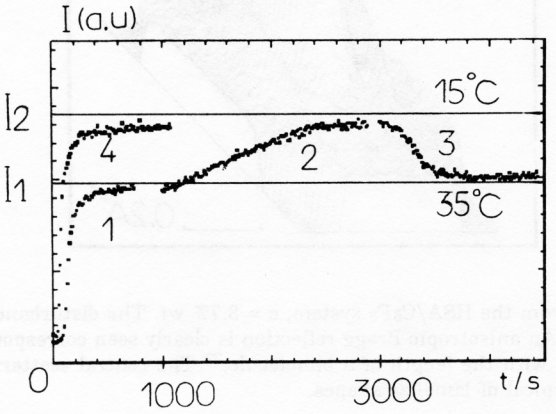

Figure 7. Kinetics of ST aggregation (c = 5.9×10^{-2}gcm^{-3}). Integrated intensity *versus* time. I is the number of neutrons within the solid angle defined by the Q-range of integration (see text) in experimental conditions where the counting time is 7 s for an irradiated volume of 80 mm^3. Integration Q-range = 0.008 Å^{-1}/0.2 Å^{-1}. Sol → gel transitions at T = 15 °C and 35 °C. The high level I_2 is proportional to the number density of rod-like aggregates at 15 °C which can be reversibly obtained by a sol → gel transition between room temperature and 15 °C (curve 4) or from a gel at 35 °C (level I_1 and curve 1) further quenched at 15 °C (curve 2). Curve 3 is a gel → gel transition obtained by annealing to 35 °C. The concentration of the ST rod-like aggregates is increased when the temperature is lowered: it is a supersaturation gel.

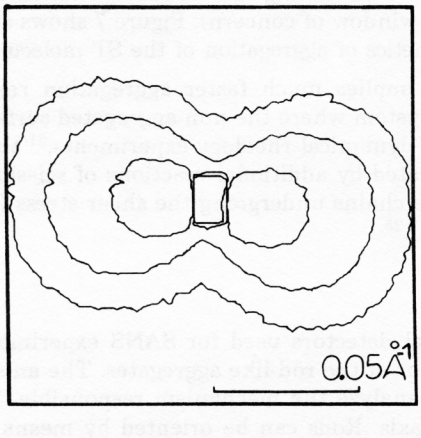

Figure 8. Anisotropic scattering: ST/C_6D_{12}, c = 5.6% wt. Two-dimensional equal intensity contours. Gel obtained in a 1 mm thick cell. For a HSA/C_6D_{12} system, circular contours characterize the isotropic scattering in an identical Q-range (not shown). The Q-range is indicated in the figure. The equivalent $Q_{||}$ axis (parallel to the shear flow) is vertical while $Q_{\perp}$ is horizontal (see text).

(8) Molecular Architecture

The structure of the surfactant-based aggregates is dependent upon both the surfactant molecular shape, its sterical specificities, and its chemical functionalities. The ST compound has a conical shape and the cross-section of the aggregates is circular. The rod-like structure is complicated by helicities with a number n_L of molecules per unit length of the aggregate of *ca.* 7 mol Å^{-1}. HSA has a linear shape and the cross-section of the aggregates is squared or rectangular. The rod-like aggregates have a lamellar internal organization involving n_L *ca.* 35 mol Å^{-1}. The simplest situation is found with the Cu-S8 system for which the rod-like aggregates require n_L *ca.* 0.22 mol Å^{-1} (corresponding to only one molecule lying per circular cross-sectional unit). The disk-like shape of the Cu-S8 molecule combined with the ability to develop coordination bondings between adjacent molecules explain the aggregation by such a simple stacking process. This mechanism is also observed in the thermotropic discotic mesophases of the bicopper alkanoates.[28] The same remark is valid for the lithium salt of HSA[29] which involves translational long-range periodicities in its thermotropic smetic liquid-crystalline phase. In contrast, if mesophases of the ST compound are unknown, xerogels[30]- from oriented gel samples in strong magnetic fields[26] exhibit nematic-like mesophases. Some structural aspects of the organogel networks are reminiscent of the related liquid-crystalline states.

As a conclusion, the present restricted overview demonstrates the large variety of structural features found with surfactant-based organogels. SANS appears to be an efficient technique for investigating both the local and long-range structural aspects of the 3d networks. Long chain-like aggregates are formed by aggregation reactions specific of the surfactants used. A polar inner core of the polar heads of the surfactants is embedded by a hydrophobic shell constituted by the hydrocarbon chains. The typical mechanical properties of these samples are partly defined by the structure of the junctions in the network: transient entanglements and crystallinity are the extreme situations found in these physical supermolecular organizations.

Acknowledgments. – It is a pleasure to thank Drs. P. Maldivi, R. Ramasseul and the ELF France Company for providing the pure derivatives and for their continuous help in the present work. The ILL is also specially thanked for providing the neutron beam facilities.

REFERENCES

1. H. F. Eicke in *Topics in Current Chemistry: Micelles*, Springer-Verlag, New York, **87** (1980) 91.
2. J. N. Israelachvili, D. J. Mitchell, and B. W. Ninham, *J. Chem. Soc. Faraday Trans. II* **72** (1976) 1525.
3. T. Kunitake, Y. Okahata, M. Shimomura, S. Yasunami, and K. Takarabe, *J. Amer. Chem. Soc.* **103** (1981) 5401.
4. J. Marignan, F. Gauthier-Fournier, J. Appell, F. Akoum, and J. Lang, *J. Phys. Chem.* **92** (1988) 440.
5. G. Porte, J. Appell, and Y. Poggi, *J. Phys. Chem.* **84** (1980) 3105.
6. S. J. Candau, E. Hirsch, R. Zana, and M. Adam, *J. Colloid Interface Sci.* **122** (1988) 430.
7. F. Reuther, G. Damaschun, C. Gernat, F. Schierbaum, B. Kettlitz, S. Radosta, and A. Nothnagel, *Colloid Polymer Sci.* **262** (1984) 6343.
8. A. Guinier and G. Fournet, in *Small angle scattering of X-rays*, Wiley, New York, 1955.
9. O. Glatter and O. Kratky, in *Small angle X-ray scattering*, Academic Press, New-York, 1982.

10. B. Cabane in *Surfactant solutions*, Surfactant Science Series, vol. **22**, R. Zana (Ed)., Marcel Dekker Inc., New-York, 1987. p. 57.
11. P. Mittelbach, *Acta Physica Austriaca* **19** (1964) 53.
12. J. des Cloizeaux, *Macromolecules* **6** (1973) 403.
13. H. Yamakawa and M. Fuji, *Macromolecules* **7** (1974) 649.
14. P. G. de Gennes, in *Scaling Concepts in Polamer Physics*, Cornell Press, Ithaca, 1979.
15. J. L. Mansot, P. Terech, and J. M. Martin, *Colloids and Surfaces* **39** (1989) 321.
16. O. Martin-Borret, R. Ramasseul, and A. Rassat, *Bull. Soc. Chimc. Fr.* (1979) 401.
17. R. L. Martin and H. Waterman, *J. Chem. Soc.* (1957) 2545; (1959) 1359.
18. P. Terech, F. Volino, and R. Ramasseul, *J. Phys. France* **46** (1985) 895.
19. P. Terech, *Progr. Colloid Polym. Sci.* **82** (1990) 263.
20. P. Terech, Colloid Polymer Sci. **269** (1991) 490.
21. P. Terech, V. Schaffhauser, P. Maldivi, and J. M. Guenet, *Europhysics Letters* **17** (1992) 515.
22. P. Terech, to be published.
23. R. H. Wade, P. Terech, E. A. Hewat, R. Ramasseul, and F. Volino, *J. Colloid Interface Sci.* **114** (1986) 442.
24. P. Terech, R. Ramasseul, and F. Volino, *J. Colloid Interface Sci.* **91** (1983) 280.
25. M. E. Cates and S. J. Candau, *J. Phys. Condens. Matter.* **2** (1990) 6869.
26. P. Terech and C. Berthet, *J. Phys. Chem.* **92** (1988) 4269.
27. P. Terech, *Liquid Crystals* **9** (1991) 59.
28. A. M. Godquin-Giroud, J. C. Marchon, D. Guillon, and A. Skoulios, *J. Phys. Lett.* **45** (1984) L681.
29. J. L. Mansot, P. Terech, and J. M. Martin, *Colloid and Surfaces* **39** (1989) 321.
30. P. Terech, *Mol. Cryst. Liq. Cryst.* **166** (1989) 29.

SAŽETAK

Agregacija surfaktanata u organskim otapalima strukturne pojave nekih fizičkih gel-umreženja sondiranih pomoću raspršenja neutrona pri malim kutovima

P. Terech

Studirani su visokoelastični gelu nalik gelatinozni sustavi surfaktanata u organskim otapalima. Raspršenje neutrona pri malim kutovima (SANS) pokazalo se kao moćna tehnika za istraživanje kako lokalnih struktura tako i struktura dugog dometa odgovarajućih 3d-umreženja. Dane su osnovne jednadžbe za raspršenje na štapićastim agregatima opaženim u tim fazama. Agregacijske reakcije uključuju specifične mehanizme za pojedine surfaktante. Nađena je značajna različitost strukturnih pojava. U svakom slučaju polarne glave surfaktanata tvore unutarnju polarnu sredinu (jezgru) koja je okružena hidrofobnom ljuskom (oblogom) ugljikovodičnih lanaca. Tipična mehanička svojstva uzoraka djelomično su određena strukturom spojišta u umreženju: prolazne smetnje i kristalne mikrodomene ekstremni su slučajevi nađeni u tim fizikalnim supermolekulskim organizacijama.